Original paper

Impact of CT texture analysis on complication rate in CT-guided liver biopsies

Maike Niebur*, Jakob Leonhardi*, Anne-Kathrin Höhn, Manuel Florian Struck, Sebastian Ebel, Gordian Prasse, Timm Denecke, Hans-Jonas Meyer

University of Leipzig, Germany

*Maike Niebur and Jakob Leonhardi contributed equally to this work.

Abstract

Aim of the study: Texture analysis derived from computed tomography (CT) involves quantitative imaging parameters characterizing possible valuable associations with clinical purposes. Their prognostic capability in patients undergoing percutaneous CT-guided liver biopsy to identify associations with postinterventional bleeding complications and biopsy success is not sufficiently explored.

Material and methods: Three hundred fifteen patients (124 female, 39%) with a mean age of 62.5 ±10.2 years underwent percutaneous CT-guided liver biopsy and were analyzed regarding clinical, procedure-related, and CT texture features.

Results: Thirty patients (9.5%) presented with bleeding after biopsy (including two requiring interventional treatment), whereas 46 patients (14.6%) had negative biopsy successes. Distance of lesion from liver capsule was statistically significantly different in patients with and without bleeding ($p = 0.015$). Several texture features were statistically significantly different between the groups, S(0,1)SumAverg having the highest significance ($p = 0.004$). Regarding unsuccessful biopsy results, liver fibrosis was the only clinical feature with statistical significance ($p = 0.049$). Only two texture features (S(4,-4)InvDfMom and Teta3) were statistically different between the groups according to the biopsy result.

Conclusions: Several CT texture features of the target lesion and the length from the capsule to the lesion were associated with bleeding complications after CT-guided percutaneous liver biopsy. This could be used to identify patients at risk at the beginning of the procedure.

Key words: CT, liver biopsy, hemorrhage.

Address for correspondence:

Dr. Hans-Jonas Meyer, Diagnostic and Interventional Radiology, University of Leipzig, Germany,
e-mail: hans-jonas.meyer@medizin.uni-leipzig.de

Introduction

The liver is a common localization of the body for focal lesions including metastases and primary tumors and harbors a variety of different focal lesions with the need of correct diagnosis [1-3]. Moreover, the incidence of malignant liver tumors has increased in recent years and consequently the need for diagnostic work up in clinical practice is increasing [3, 4].

Cross-sectional imaging comprising computed tomography (CT) and magnetic resonance imaging (MRI) can detect and characterize liver lesions, but in most cases, a definite diagnosis is needed by bioptic specimen and histopathology evaluation [2, 5].

Image-guided biopsy with a percutaneous approach is the established method for tissue sampling in routine clinical practice [6]. In most centers, sonography and CT guidance is employed to display the target lesion and the biopsy needle sufficiently [7]. CT

guidance allows for a better visualization of the needle tip and might provide a greater overview regarding the anatomical structures during the intervention [8]. However, this comes with a greater cost of CT guidance, with an estimated 3.15 times higher cost [9]. However, the CT images could be further evaluated by radiomics analysis to further provide prognostic information.

The overall complication rate of liver biopsies was reported to range from 0.4% to 1.7% with an estimated mortality of 0.11% for this procedure [7, 10, 11]. Complications of the procedure can range from severe pain, hypotension, bleeding, and fluid collections to pneumothorax [10].

A recent study identified an overall complication rate of 1.6% of 2405 liver biopsies with sonography guidance [10]. Of these, 21 patients (0.9%) and 17 patients (0.7%) had postinterventional hemorrhage with hemoperitoneum and liver hematoma, respectively. However, only underlying factors for general post-biopsy complications were investigated in this study and a subanalysis for postinterventional hemorrhage was not provided [10]. To identify patients at risk for hemorrhage after biopsy is of clinical importance.

Texture analysis could be used to provide a quantitative imaging analysis, which can characterize radiological images beyond the basic imaging evaluation [12-15]. Using this approach, microstructural changes of tissues can be reflected with imaging modalities, as shown in several oncological studies [16-18]. CT texture analysis might be directly influenced by the underlying tumor structure and by this approach enables a method to better characterize tumor lesions.

Presumably, it could also help to characterize target lesions with a risk of bleeding complications and therefore potentially better stratify patients at risk for complications undergoing CT-guided liver biopsy.

The purpose of the present analysis was to use quantitative imaging features to predict postinterventional bleeding complications and negative biopsy success in patients undergoing percutaneous CT-guided liver biopsy.

Material and methods

Patient acquisition

After approval of the Ethics Committee of the Medical Faculty of the University of Leipzig, Germany (register no. 344-2007) all patients undergoing CT-guided liver biopsy at the University Hospital Leipzig between the years 2012 and 2021 were analyzed in a retrospective observational study. Written informed consent was obtained from all patients before CT-guided biopsy.

Clinical parameters

Clinical parameters of the patients were retrieved from the medical records. Anamnestic presence of prior cancer diagnosis, diabetes mellitus, arterial hypertension, clinical cholestasis were extracted from the records. Steatosis and fibrosis of the liver were retrieved from the biopsy report.

CT-guided biopsy

All biopsies investigated in this study were performed by interventional-trained radiologists with at least two years of general experience in interventional radiology. The procedure plan (comprising the position and the needle pathway) was calculated using previous CT images. As puncture-related parameters several distances were measured on axial slices: the distance of needle entry to the liver capsule, distance of the lesion to the liver capsule, the distance of the lesion to the needle entry of the liver. The needle angle of the entry of the biopsy was measured to the horizontal plane. The maximum size of the target lesion was measured with 2 perpendicular diameters on the largest, representative slice. Finally, the duration of the biopsy was defined from the planning scan to the last control sequence after needle removal.

All interventions were performed with the same CT scanner (16-slice CT scanner, Brilliance Big Bore, Philips, Hamburg, Germany). Typical CT parameters were set as: 100 kVp, 125 mAs, slice thickness 1 mm, pitch, 0.9.

All biopsies were performed after confirmation of absence of coagulation disorders (platelet count was at least 50,000/mm^3, activated partial thromboplastin time [aPTT] $\leq$ 50 seconds and prothrombin time (Quick) > 50%). The procedure started with disinfection of the skin and local anesthesia with 10 ml of lidocaine 1% (Xylocitin, Jenapharm, Germany). A coaxial 18-gauge biopsy system of a 2 cm throw length needle was used (Bard Mission, Bard Medical, Covington, GA 30014, USA or Biopince, Argon Medical Devices, Athens, TX 75751, USA). During the procedure, CT images were used to validate the accurate localization of the needle tip to reach the target lesion correctly. After removal of the biopsy needle, CT images over the liver were acquired to rule out post-interventional bleeding complications. Hematoma width was measured on one slice using the perpendicular diameter. The diagnostic outcome of the biopsy was determined by the pa-

Maike Niebur, Jakob Leonhardi, Anne-Kathrin Höhn, Manuel Florian Struck, Sebastian Ebel, Gordian Prasse, Timm Denecke, Hans-Jonas Meyer

thology report and with the need of re-biopsy during the clinical course.

Texture analysis

Computed tomography images were further analyzed with the dedicated software MaZda (version 4.7, available at http://www.eletel.p.lodz.pl/mazda/) [19, 20]. A region of interest (ROI) was drawn on the largest slice of the target lesion. The ROI was drawn within the liver lesion with 2 mm distance to the adjacent parenchyma. Texture analysis measurements were blindly taken for the bioptic and clinical results. For each ROI, gray-level (μ) normalization was utilized to $\mu \pm 3$ standard deviations to reduce the influence of contrast and brightness variation on the texture features, as performed previously [16, 17]. Texture features of various groups were extracted for each patient including histogram parameters, second order texture features of different groups comprising co-occurrence matrix run-length matrix, absolute gradient, autoregressive model (theta 1 to 4, sigma), and wavelet transform features. Altogether, 279 texture features were calcu-

lated in all lesions. Two representative cases of the patient sample are shown in Figure 1 with the drawn ROI.

Statistical analysis

Collected data were primarily assessed with descriptive statistics. Group differences were analyzed with the Mann-Whitney U test and Fisher's exact test. Receiver operating characteristics curve (ROC) with area under the curve (AUC) analyses were used to investigate diagnostic accuracy for the investigated parameters. Furthermore, a binary logistic regression model was conducted to provide a multivariate prediction model. P-values below 0.05 were considered statistically significant. All analyses were performed with SPSS (IBM, Version 25.0; Armonk, NY, USA).

Results

The patient sample consisted of 315 patients overall (124 female patients, 39%) with a mean age of 62.6 $\pm$10.2 years. Thirty patients (9.5%) of the total
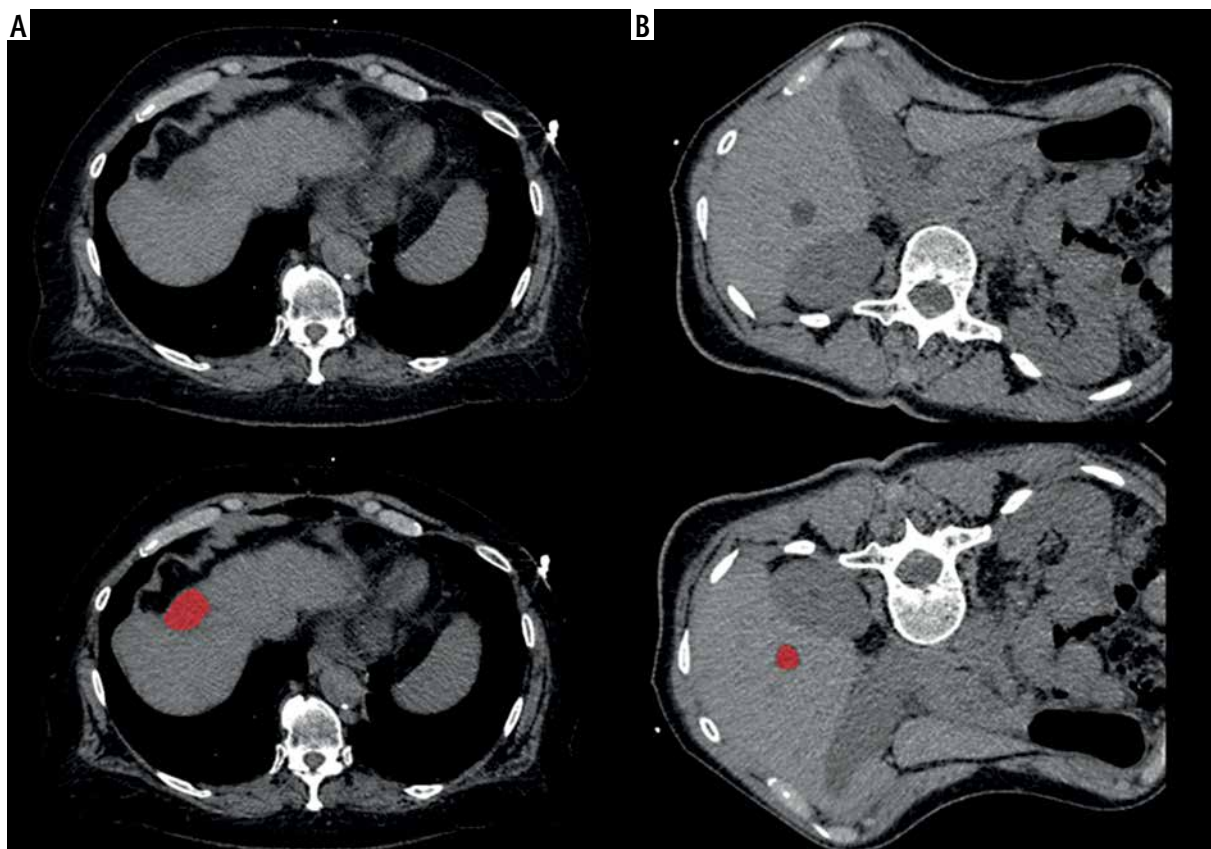
Fig. 1. Representative cases of the patient sample. **A)** 68-year-old female patient, no steatosis, no fibrosis, diagnostic biopsy with benign result, platelet count 316,000/µl, distance to liver capsule 0 mm, no hemorrhage. **B)** 61-year-old female patient, steatosis degree 5%, minimal fibrosis, non-diagnostic biopsy, platelet count 81,000/µl, distance to liver capsule 13 mm, no hemorrhage

Table 1. Clinical features in cases with and without post-biopsy hemorrhage

Clinical features	Hemorrhage (n = 30) n (%) or mean ±SD	No hemorrhage (n = 285) n (%) or mean ±SD	P-value
Gender (female)	13 (43.3)	105 (36.8)	0.58
Age (years)	63.70 ±7.97	62.58 ±13.64	0.89
Prior cancer diagnosis	9 (30)	105 (36.8)	0.46
Malignant pathology	22 (73.3)	208 (73.0)	0.96
Cholestasis	5 (16.7)	39 (13.7)	0.63
Steatosis	0.11 ±0.17	0.14 ±0.20	0.64
Fibrosis	18 (60)	207 (72.6)	0.24
Diabetes mellitus	8 (26.7)	98 (34.4)	0.47
Arterial hypertension	18 (60)	157 (55.1)	0.64
aPTT (s)	30.14 ±5.22	29.84 ±5.18	0.81
Platelet count (10^3/µl)	207.40 ±119.89	252.21 ±135.29	0.05
Quick (%)	89.27 ±17.89	86.21 ±17.32	0.23

Table 2. Biopsy procedure features in cases with and without post-biopsy hemorrhage

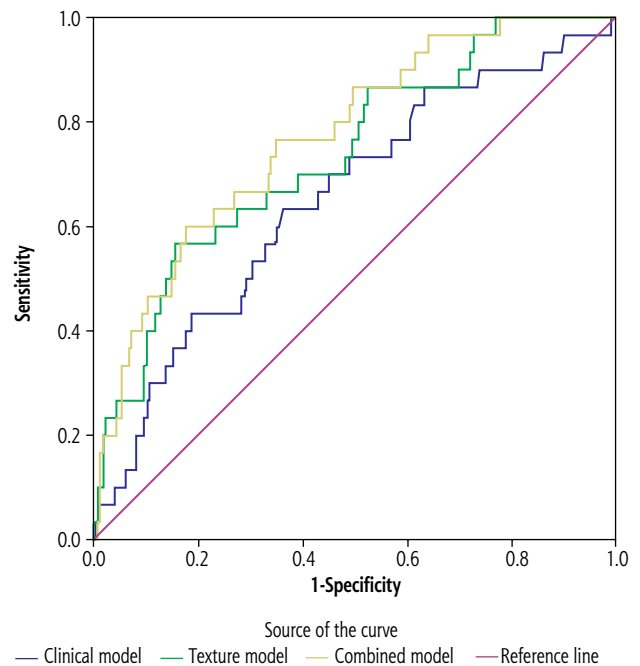| Puncture features	Hemorrhage (n = 30) mean ±SD or n (%)	No hemorrhage (n = 285) mean ±SD or n (%)	P-value
Distance of needle entry to liver capsule (mm)	16.20 ±10.70	14.17 ±8.18	0.39
Distance lesion from liver capsule (mm)	9.41 ±11.56	5.40 ±9.27	0.015
Distance of lesion to needle entry (mm)	41.00 ±18.02	44.09 ±27.62	0.96
Lesion size (mm²)	1238.33 ±1669.51	1398.08 ±2294.97	0.87
Needle angle	62.27 ±21.23	63.07 ±17.69	0.93
Duration of intervention (minutes)	18.93 ±14.14	17.40 ±11.03	0.99
Success of biopsy	25 (83.3)	244 (85.6)	0.72

Table 3. Overview of statistically significant texture features in comparison between cases with post-biopsy hemorrhage and without hemorrhage. The features in bold letters were added to the multivariate model for prediction of hemorrhage

Texture features	Hemorrhage (n = 30)	No hemorrhage (n = 285)	P-value
S(1,0)SumAverg	64.38 ±0.43	64.12 ±0.53	0.008
S(0,1)SumAverg	64.43 ±0.46	64.13 ±0.54	0.004
S(1,1)SumAverg	64.39 ±0.52	64.10 ±0.57	0.016
S(1,-1)SumAverg	64.37 ±0.47	64.10 ±0.57	0.007
S(2,0)SumAverg	64.35 ±0.55	64.06 ±0.64	0.020
S(0,2)SumAverg	64.34 ±0.63	64.09 ±0.64	0.014
S(2,-2)SumAverg	64.34 ±0.62	64.04 ±0.69	0.020
S(3,0)SumAverg	64.33 ±0.66	64.02 ±0.74	0.047
S(0,3)SumAverg	64.44 ±0.78	64.07 ±0.74	0.039
S(3,-3)Contrast	197.22 ±26.46	208.42 ±31.46	0.044
S(4,0)Contrast	195.50 ±28.24	209.24 ±31.77	0.018
S(4,0)Correlat	0.10 ±0.12	0.04 ±0.14	0.029
S(4,0)InvDfMom	0.09 ±0.01	0.08 ±0.01	0.012
S(4,0)DifVarnc	70.68 ±10.39	75.80 ±11.51	0.014
S(5,0)Contrast	201.14 ±22.00	212.85 ±28.26	0.043
S(5,0)DifVarnc	72.12 ±8.36	76.94 ±10.13	0.011
WavEnLL_s-1	17,456.03 ±259.67	17,299.61 ±403.94	0.014

Fig. 2. ROC curves of the prediction models of hemorrhage based on clinical and texture features

sample had post-interventional bleeding complications, of which the majority (28 patients) were cases of minor bleeding without the need for blood transfusion or emergency intervention. In two cases (0.6%), severe bleeding resulted in the necessity of emergency endo-

vascular treatment – in one case the origin of the hemorrhage was an intercostal artery, and in the other case, a bleeding arterial liver vessel within the biopsy tract. The mean width of the perihepatic hematoma was 13 mm, ranging from 4.6 mm to 92.6 mm.

Differences between patients with and without hemorrhage were found in platelet count and the distance of the target lesion to the liver capsule (Tables 1 and 2).

Significant differences of texture features of the punctured lesions between patients with and without bleeding complications are shown in Table 3.

Multivariate model regarding prediction of hemorrhage

A multivariate model was developed based on the significant clinical features (n = 1), procedure-related features (n = 1) and the most significant texture features (n = 6) to predict bleeding complications. The clinical model resulted in an AUC of 0.65 (95% CI: 0.55-0.76). The texture-based model yielded comparably superior predictive power with an AUC of 0.74 (95% CI: 0.65-0.83), while the combined model resulted in an AUC of 0.77 (95% CI: 0.69-0.86). The corresponding ROC graphs are displayed in Figure 2.

Success of biopsy

In 269 (85.4%) cases, the biopsy procedure was successfully performed. Differences of clinical and puncture features of the punctured lesions between patients with and without success of biopsy are shown in Tables 4 and 5. Three parameters were associated with biopsy success: In patients with histological fibrosis, there was a lower rate of biopsy success (69.9% vs. 80.43% in non-fibrotic patients, p = 0.049). Two texture features, S(4,-4)InvDfMom and Teta3, were also statistically significantly different between groups (p = 0.035 and p = 0.045, respectively).

Table 4. Clinical features in cases with and without diagnostic biopsy

Clinical features	Diagnostic biopsy (n = 269) n (%) or mean ±SD	No diagnostic biopsy (n = 46) n (%) or mean ±SD	P-value
Gender (female)	101 (37.5)	22 (47.8)	0.19
Age (years)	62.38 ±13.19	64.80 ±13.02	0.32
Prior cancer diagnosis	102 (37.8)	12 (26.1)	0.12
Cholestasis	34 (12.6)	10 (21.7)	0.12
Steatosis	0.13 ±0.19	0.18 ±0.23	0.06
Fibrosis	188 (69.9)	37 (80.43)	0.049
Diabetes mellitus	89 (47.3)	17 (37.0)	0.62
Arterial hypertension	151 (56.1)	26 (56.5)	0.96
aPTT (s)	29.86 ±5.35	29.92 ±4.02	0.24
Platelet count	247.36 ±133.81	251.11 ±139.00	0.74
Quick (%)	86.89 ±17.40	84.26 ±17.22	0.96

Multivariate model regarding prediction of diagnostic biopsies

A multivariate model was developed based on these 3 parameters to predict the success of the biopsies as defined by diagnostic results. The model based on CT texture features only yielded an AUC of 0.50 (95% CI: 0.40-0.59), which was not predictive of a diagnostic biopsy result.

Discussion

The present analysis suggests that quantitative CT imaging features are associated with postinterventional bleeding after CT-guided liver biopsy.

Furthermore, the rate of successful biopsy results are in line with previous studies. A recent study investigating the importance of Lipiodol marking of liver lesions had a success rate of 73.1% overall [21]. Moreover, liver cirrhosis and the entity of the lesion had no influence on success rate, contrary to the present results [21]. Other authors reported a success rate of 100% in 767 patients [22]. However, most published reports range between these values [23-25].

Despite its low risk profile, several complications have been reported [7, 10]. Among them, and most severe, is bleeding with a potentially lethal outcome. In a recent study of more than 300 patients, the overall complication rate was 4.6% [23]. Four cases of this patient sample had severe hemorrhage needing angiographic treatment (1.4% of the patient sample) [23]. In our case sample, two cases required endovascular treatment of the severe hemorrhage, which is slightly lower compared with the patient sample of Hoffmann *et al.* [23].

Table 5. Puncture features in cases with and without diagnostic biopsy

Puncture features	Diagnostic biopsy (n = 269)	No diagnostic biopsy (n = 46)	P-value
Distance of needle entry to liver capsule (mm)	14.66 ±8.77	12.83 ±6.30	0.39
Distance lesion from liver capsule (mm)	5.97 ±9.95	4.91 ±7.23	0.90
Distance of lesion to needle entry (mm)	43.87 ±26.33	45.70 ±29.50	0.95
Lesion size (mm²)	1404.23 ±2326.24	1174.72 ±1409.41	0.33
Needle angle	62.67 ±18.06	63.96 ±17.66	0.61
Duration of intervention (min)	17.89 ±11.49	15.30 ±10.58	0.11

The overall identified rate of 9.5% of postinterventional hemorrhage in the present cohort is relatively high, when compared to others studies. In a study on 129 biopsies of hepatocellular carcinomas, two patients (1.6% of cases) showed post-biopsy bleeding [26]. A large older study utilizing 9212 sonography-guided liver biopsies reported 11 fatal (0.11% and 22 nonfatal hemorrhages (0.24%) [11]. Another representative study of 68,276 biopsies from 1973 to 1983 reported fatal outcomes in 9 of 100,000 cases due to hemorrhage [6]. However, Midia et al. reported bleeding of any kind in up to 10.9% of cases after liver biopsies, which is comparable with the present data [8]. A very low complication rate was reported by a recent Italian study investigating 800 ultrasonography-guided biopsies with a moderate hemorrhagic complication rate of only 0.75% [27].

The definition of relevant postinterventional bleeding may be different depending on the study criteria. We included every postinterventional hyperdense fluid surrounding the liver, regardless of clinical presentation. This might explain our higher frequency of bleeding compared with studies utilizing ultrasonography for the evaluation of clinical symptomatic patients.

In the literature, various associations have been identified with post-biopsy bleeding.

Age over 50 years was a factor found to be associated with a higher rate of bleeding in the study by van der Poorten et al. [28]. We did not identify differences regarding age in our patient sample.

Another factor was abnormal platelet count and INR, which was reported by Myers et al. [29]. In the present analysis, the difference in platelet count between the patient groups almost reached statistical significance.

Lesion-dependent factors have also been evaluated in the literature [30-32]. There were no reported differences between biopsies of the parenchyma compared to focal lesions [30-32]. In the present study, only focal targeted biopsies were investigated.

There are sparse data regarding the angle of the biopsy needle or length inside the liver parenchyma during the biopsy. The length from the liver capsular to the lesion is a significant factor for post-biopsy hemorrhage and should be considered as a potential risk factor.

Moreover, the present results can provide the potential benefit of texture analysis of the target lesion to identify patients at risk. Several texture features derived from the co-occurrence matrix run-length matrix group were different between patients with and without post-interventional hemorrhage. These features reflect the heterogeneities of the grey levels of the target lesion in a spatial manner [15]. Presumably, by using this approach it is possible to better characterize tumors with a higher potential for bleeding complications.

It is well established that CT texture features might reflect the microstructure of tumors, as defined by cellularity and cell sizes [16]. The rationale is that the grey-level scales of the CT images are directly influenced by the histopathologic underlying microstructure of the tumors and this approach enables non-invasive tissue characterization by imaging. In other studies, CT texture analysis was associated with grading and proliferative potential of the tumor indicating its capability to also reflect tumor aggressiveness [14, 17].

However, the identified diagnostic accuracy is still relatively low, which might hinder the translation into clinical practice. As discussed above, lesion type and underlying histopathology might only have a small impact on the bleeding risk of the patient [30-32]. Another important aspect is that MRI might be able to characterize small lesions even in cirrhotic patients and might reduce the need for invasive liver biopsy [33]. This can also be assessed by contrast-enhanced ultrasound, which is able to characterize even small hepatocellular carcinomas, when the typical contrast media enhancement is present [34].

Further studies should assess which unclear liver lesions profit the most from CT texture analysis prior to liver biopsy depending on their characteristics in MRI and ultrasonography.

Moreover, CT texture analysis was not able to reflect diagnostic success of the biopsy. However, the investigated clinical parameters and procedure-related parameters were also not associated with the biopsy outcome. Only the presence of fibrosis was statistically significantly associated, which might be related to difficult targeting of the lesion in fibrotic livers.

The present analysis has some limitations. First, it is a retrospective study with known inherent bias. Second, although in all cases an 18G needle was used for the biopsy, the needle length varied slightly due to the localization of the target lesion. Third, all patients with post-biopsy bleeding were included in the present analysis, independently of clinical presentation. There might be other associations of the investigated parameters in clinically more severely deteriorated patients. Yet, due to the retrospective study design, it was not possible to obtain enough clinical information to perform a subanalysis for these patients. This also included the diagnosis of liver cirrhosis of the investigated patients. Due to the obtained clinical information, we could only adjust for liver fibrosis within the biopsy specimen but we could not adjust for the effect of liver

cirrhosis, which could have an influence on the bleeding risk and on the investigated CT texture features.

In conclusion, several CT texture features of the target lesion and the length from the capsule to the lesion were associated with bleeding complications after CT-guided percutaneous liver biopsy. These features could be used to identify patients at risk at the beginning of the procedure.

Disclosure

The authors declare no conflict of interest.

References

1. Mielgo A, Schmid MC. Liver tropism in cancer: The hepatic metastatic niche. Cold Spring Harb Perspect Med 2020; 10: a037259.
2. Ariff B, Lloyd CR, Khan S, et al. Imaging of liver cancer. World J Gastroenterol 2009; 15: 1289-300.
3. Llovet JM, Burroughs A, Bruix J. Hepatocellular carcinoma. Lancet 2003; 362: 1907-1917.
4. McGlynn KA, Petrick JL, El-Serag HB. Epidemiology of hepatocellular carcinoma. Hepatology 2021; 73 Suppl 1: 4-13.
5. Haj-Mirzaian A, Kadivar A, Kamel IR, Zaheer A. Updates on imaging of liver tumors. Curr Oncol Rep 2020; 22: 46.
6. Piccinino F, Sagnelli E, Pasquale G, Giusti G. Complications following percutaneous liver biopsy. A multicentre retrospective study on 68,276 biopsies. J Hepatol 1986; 2: 165-173.
7. Neuberger J, Patel J, Caldwell H, et al. Guidelines on the use of liver biopsy in clinical practice from the British Society of Gastroenterology, the Royal College of Radiologists and the Royal College of Pathology. Gut 2020; 69: 1382-1403.
8. Midia M, Odedra D, Shuster A, et al. Predictors of bleeding complications following percutaneous image-guided liver biopsy: a scoping review. Diagn Interv Radiol 2019; 25: 71-80.
9. Kliewer MA, Sheafor DH, Paulson EK, et al. Percutaneous liver biopsy: a cost-benefit analysis comparing sonographic and CT guidance. AJR Am J Roentgenol 1999; 173: 1199-1202.
10. Maheux A, Purcell Y, Harguem S, et al. Targeted and non-targeted liver biopsies carry the same risk of complication. Eur Radiol 2019; 29: 5772-5783.
11. McGill DB, Rakela J, Zinsmeister AR, Ott BJ. A 21-year experience with major hemorrhage after percutaneous liver biopsy. Gastroenterology 1990; 99: 1396-1400.
12. Lubner MG, Smith AD, Sandrasegaran K, et al. CT texture analysis: Definitions, applications, biologic correlates, and challenges. Radiographics 2017; 37: 1483-1503.
13. Lambin P, Rios-Velazquez E, Leijenaar R, et al. Radiomics: extracting more information from medical images using advanced feature analysis. Eur J Cancer 2012; 48: 441-446.
14. Aerts HJ, Velazquez ER, Leijenaar RT, et al. Decoding tumour phenotype by noninvasive imaging using a quantitative radiomics approach. Nat Commun 2014; 5: 4006.
15. Incoronato M, Aiello M, Infante T, et al. Radiogenomic analysis of oncological data: A technical survey. Int J Mol Sci 2017; 18: 805.
16. Meyer HJ, Hamerla G, Höhn AK, Surov A. CT texture analysis-correlations with histopathology parameters in head and neck squamous cell carcinomas. Front Oncol 2019; 9: 444.
17. Meyer HJ, Leonhardi J, Höhn AK, et al. CT texture analysis of pulmonary neuroendocrine tumors-associations with tumor grading and proliferation. J Clin Med 2021; 10: 5571.
18. Canellas R, Burk KS, Parakh A, Sahani DV. Prediction of pancreatic neuroendocrine tumor grade based on CT features and texture analysis. AJR Am J Roentgenol 2018; 210: 341-346.
19. Strzelecki M, Szczypinski P, Materka A, Klepaczko A. A software tool for automatic classification and segmentation of 2D/3D medical images. Nucl Instrum Methods Phys Res A 2013; 702: 137-140.
20. Szczypiński PM, Strzelecki M, Materka A, Klepaczko A. MaZda – a software package for image texture analysis. Comput Methods Prog Biomed 2009; 94: 66-76.
21. Langenbach MC, Vogl TJ, Buchinger A, et al. CT-guided biopsies of unspecified suspect intrahepatic lesions: pre-procedure Lipiodol-marking improves the biopsy success rate. Radiol Oncol 2023; 57: 158-167.
22. Thanos L, Zormpala A, Papaioannou G, et al. Safety and efficacy of percutaneous CT-guided liver biopsy using an 18-gauge automated needle. Eur J Intern Med 2005; 16: 571-574.
23. Hoffmann P, Cyrany J, Kopecky J, et al. Percutaneous CT-guided biopsy of focal liver lesions – long-term experience with more than 300 procedures. J Gastrointestin Liver Dis 2023; 32: 197-205.
24. Ma X, Arellano RS, Gervais DA, et al. Success of image-guided biopsy for small (≤ 3 cm) focal liver lesions in cirrhotic and noncirrhotic individuals. J Vasc Interv Radiol 2010; 21: 1539-1547.
25. Knöpfle E, Bohndorf K, Wagner T. Does the core biopsy of solid liver lesions permit an exact histological classification? Results of a prospective study under routine clinical conditions. Rofo 1997; 167: 406-411.
26. Ch Yu S, Metreweli C, Lau WY, et al. Safety of percutaneous biopsy of hepatocellular carcinoma with an 18 gauge automated needle. Clin Radiol 1997; 52: 907-901.
27. Mulazzani L, Terzi E, Casadei G, et al. Retrospective analysis of safety of ultrasound-guided percutaneous liver biopsy in the 21st century. Eur J Gastroenterol Hepatol 2021; 33: e355-e362.
28. van der Poorten D, Kwok A, Lam T, et al. Twenty-year audit of percutaneous liver biopsy in a major Australian teaching hospital. Intern Med J 2006; 36: 692-699.
29. Myers RP, Fong A, Shaheen AA. Utilization rates, complications and costs of percutaneous liver biopsy: a population-based study including 4275 biopsies. Liver Int 2008; 28: 705-712.
30. Mueller M, Kratzer W, Oeztuerk S, et al. Percutaneous ultrasonographically guided liver punctures: an analysis of 1961 patients over a period of ten years. BMC Gastroenterol 2012; 12: 173.
31. Atwell TD, Smith RL, Hesley GK, et al. Incidence of bleeding after 15,181 percutaneous biopsies and the role of aspirin. AJR Am J Roentgenol 2010; 194: 784-789.
32. Westheim BH, Ostensen AB, Aagenaes I, et al. Evaluation of risk factors for bleeding after liver biopsy in children. J Pediatr Gastroenterol Nutr 2012; 55: 82-87.
33. Granito A, Galassi M, Piscaglia F, et al. Impact of gadoxetic acid (Gd-EOB-DTPA)-enhanced magnetic resonance on the non-invasive diagnosis of small hepatocellular carcinoma: a prospective study. Aliment Pharmacol Ther 2013; 37: 355-363.
34. Leoni S, Piscaglia F, Granito A, et al. Characterization of primary and recurrent nodules in liver cirrhosis using contrast-enhanced ultrasound: which vascular criteria should be adopted? Ultraschall Med 2013; 34: 280-287.